DYNAMIC MODELING AND PREDICTION OF CYTOTOXICITY ON MICROELECTRONIC CELL SENSOR ARRAY

Biao Huang [a], James Z. Xing [b],

[a] *Dept. of Chemical and Materials Engg., Uinv. of Alberta, Edmonton, AB, Canada, T6G 2G6*

[b] *Department of Laboratory Medicine and Pathology, University of Alberta, Edmonton, Alberta, Canada T6G 2S2*

Abstract

A real-time cell electronic sensing (RT-CES) system has been used for label-free dynamic measurements of cell responses to toxicant. Cells are grown onto the surfaces of the microelectronic sensors. Changes in cell number expressed as cell index (CI) have been recorded on-line as time series. The CI data are used for dynamic modeling or parameter estimation for cell cytotoxicity process. We consider two dynamic modeling approaches, namely data based system identification and first principle modeling. It is shown that data based system identification can provide a quick solution for the cytotoxicity dynamic models and is effective for short term predictions. It, however, can be poor for long term predictions, particularly if there is no output correction, i.e. when the model is used for simulation. In view of this, the first principle modeling approach by considering fundamental physical principles such as toxicant transport is explored. For long term prediction or simulation, the prediction performance for some of cytotoxicity process is dramatically improved using the models obtained from the latter approach. This happens only if the underlying mechanism is truly understood. Through several cytotoxicity modeling and validation studies, it is shown that the blackbox modeling and first-principle modeling both should be considered in challenging modeling problems such as the cytotoxicity. Pros and cons of the two modeling approaches are discussed.

Key words: Cytotoxicity, cell modeling, dynamic modeling, parameter estimation, system identification

⋆ Corresponding author B. Huang. Tel. +1-780-4929016. Fax +1-780-4922881.
Email addresses: biao.huang@ualberta.ca (Biao Huang), jzxing@ualberta.ca (James Z. Xing).

INTRODUCTION

Cytotoxicity is the degree to which an agent possesses a specific toxic action on living cell referring to cells killing, cell lysis and certain cellular pathological changes, such as cellular morphological and adhesion change, induced by toxic agents.

When exposing to toxic compounds, cells undergo physiological and pathological changes, including morphological dynamics, an increase or decrease in cell adherence to the extracellular matrix, cell cycle arrest, DNA damage, apoptosis and necrosis (Xing *et al.*, 2005). Such cellular changes are dynamic and depend largely on cell types, the nature of a chemical compound, compound concentration, and compound exposure duration. In addition, certain cellular changes, such as morphological dynamics and adhesive changes, which may not lead to ultimate cell death, are transient and occur only at early or late stages of toxicant exposure. Modeling such diverse information sets is challenging at the analytical level. Understanding of underlying mechanism plus experiments has to be resorted to.

Dynamic information of cells provides an additional dimension and insight into explanation of cell behavior such as cytotoxicity comparing with conventional fixed point observations method such as cell viability. Dynamic responses are typically described by dynamic models. These models can take many different forms, such as a state space model, transfer function, neural net, fuzzy logic etc. To obtain the dynamic model, one usually has to perform dynamic experiments, determine model structure, estimate model parameters, and validate the model (Soderstrom and Stoica, 1989). This complete procedure is known as system identification in systems and control literature (Ljung, 1999).

Time series expression experiments are an increasingly popular method for studying a wide range of biological systems because the information of dynamic behavior in biological system provided by such experiments is essential for biology system analysis. Time series analysis of biological system may be classified into a hierarchy of four analysis levels: experimental design, data analysis, pattern recognition and networks(Bar-Joseph, 2004). This paper will focus on the data analysis aspect for dynamic modeling.

The first application of time series is for system identification. However, models obtained from system identification have limit validity (Soderstrom and Stoica, 1989). They are usually valid within the range of experiments and their prediction performance can deteriorate quickly outside the experiment range, particularly for highly nonlinear processes. These models give little physical insight and in most cases the parameters of the model have no direct physical meaning. The parameters are used only as tools to give a good description

of the system's overall behavior within certain range. Nevertheless, they are relatively easy to construct and use, particularly for short term prediction or for control purpose, and thus are widely used in systems and control.

For a long term prediction, the first principles of cytotoxicity and its dynamic behavior have to be investigated, and the underlying mechanism has to be understood. However, most available contributions in cytotoxicity are empirical and models developed often represent steady state or a few intermediate points of the cytotoxicity process. In a related area of pharmacokinetics and pharmacodynamics where the effect of drug is of main interest, however, several mathematical models have been developed to predict the dynamic behavior of drugs in vitro. In (El-Kareh and Secomby, 2005), a mathematical model is presented for the cellular uptake and cytotoxicity of the anticancer drug doxorubicin. The model assumes sigmoidal, Hill-type dependence of cell survival on drug-induced damage. Drug-induced damage is expressed as the sum of two terms, representing the peak values over time of concentrations of intracellular and extracellular drugs. Hill equation is an empirical relation representing cell survival rate and peak values of cell concentration represent only single points of the dynamic profile. In (Lankelma *et al.*, 2003), cell proliferation is expressed dynamically as $N = N_0 exp(kt)$, where N is cell papulation, N_0 is cell papulation at time 0. The parameter k has an expression $k = b \log(N_\infty/N_0)$ (b is a constant) without the presence of drug and $k = k_0 \exp(-\xi)$ with the presence of drug. With the presence of drug the term ξ is a complicated integral of drug accumulation in the cell. These expressions are derived on the assumption that cell population is dependent on the accumulation of drug inside the cells.

There are several other mathematical models for drug dynamics, but are similar to either (El-Kareh and Secomby, 2005) or (Lankelma *et al.*, 2003). The basic principle is that cell population depends on the area under the concentration curve. For example, in (Doroshow, 1996), antitumor effect of drugs is assumed to be a function of Area Under the drug Concentration time curve (AUC). In (Ozawa *et al.*, 1980), it was proposed to fit an exponential (dynamic) model for cytotoxic effect of doxorubicin to data with the form of $S = exp(-ktc_e)$ where S is cell survival relative to control at time t, c_e is extracellular drug concentration. In (Millenbaugh *et al.*, 2000), a cell-killing mechanism dependent on $c^n t$ was proposed, where c is drug concentration. There is evidence that drugs can kill cells without actually entering them; intracellular drug is nevertheless believed to make a significant contribution to cell killing (Gewirtz, 1999).

Instead of relying on empirical correlations, area under concentration curve (AUC), or integration of $c^n t$, in this paper, we consider cytotoxicity modeling according to fundamental transport principles and mechanism of toxicant effect. We will first assume a mechanism according to certain a priori knowledge

of cell killing pathway, and then model structures are derived analytically with certain unknown parameters. The parameters are then estimated from experiment data, and cross verified by independent data sets. The validity of the mechanism can be determined through the cross validation. If the model fails cross validation test, a new mechanism is assumed and the procedure repeats.

Regardless system identification or first-principle modeling with parameter estimation, the dynamic experiment is the first step and the most important step to ensure the quality of the modeling or parameter estimation. However, the dynamic monitoring of cytotoxicity is difficult to achieve in most of conventional cell based assays because they need chemical or radiation indicators that may kill or disturb target cells. For dynamic detection of a broad range of physiological and pathological responses to toxic agents in living cells, Xing et al (2005) has developed an automatic, real-time cell electronic sensing (RT-CES) system that is used for cell-based assay. This system has advantage of greater precision of dynamic monitoring of cytotoxicity than experiments performed in classical pharmacokinetics and pharmacodynamics.

In this paper, a dynamic modeling framework for the cytotoxicity will be established. The cell index (CI) data obtained from several cytotoxicity experiments based on RT-CES will be analyzed. According to the previous study (Xing *et al.*, 2005), the CI values as determined on the RT-CES system were found to be linearly correlated with cell numbers over the range between 125 and 16000 cells, having a correlation coefficient of 0.995. For viable cell counting and quantification, the data generated on the RT-CES system are consistent with that obtained for the MTT assay. It will be shown in this paper that the dynamic model can play an important role in analyzing intrinsic cell behavior and predict the trajectory of its progress (growth or death) over considerable time horizon.

DYNAMIC MODELS AND PREDICTIONS

There are numerous ways to represent dynamic models. In this paper the following model structures are considered:

First-principle model: This is the most commonly used model based on the first principles of underlying process. The model to be considered in this paper takes the following form:

$$\frac{dy(t)}{dt} = f(u(t), y(t), t) + e(t)$$

where $f()$ is a nonlinear function and has to be derived from first principles, and $e(t)$ is the measurement noise.

Nonlinear autoregressive with exogenous input (NARX): This is frequently used dynamic model in data-based nonlinear system identification. We consider the following form of NARX model in difference equation form:

$$y_t = f(y_{t-1}, \cdots, y_{t-p}, u_t, \cdots, u_{t-q}) + e_t$$

where the structure of $f()$ is unknown and has to be identified from data.

Two types of predictors will be considered, namely k-step ahead predictor and infinite-step ahead predictor. Predictors are derived from dynamic models. They serve for two purposes: 1) Used for dynamic prediction of future outputs based on current available information. 2) The predicted outputs from the predictors can be used to verify models. There are two types of model validations used in this work: 1) Validation using the same experiment data to verify the model. This type of validation has been used frequently in the literature, which, strictly speaking, is not validation. We call this type of validation as self validation. 2) Validation using independent data to verify the model. We call it cross validation.

Models can be verified according to either k-step ahead prediction or infinite-step ahead prediction, with latter being a more rigorous criterion.

k-step ahead prediction is given by

$$\hat{y}_{t+k|t} = p(y_t, y_{t-1}, \cdots; u_{t+k}, u_{t+k-1} \cdots)$$

where $\hat{y}_{t+k|t}$ is prediction of y_{t+k} based on all information available at time t. One may notice that the prediction has used measured output up to time t, which may be considered as a correction/update of the prediction. Thus a model is easier to pass this type of validations particularly when the prediction horizon k is small and output response is smooth.

Infinite step ahead prediction or simulation is given by

$$\hat{y}_{t+k} = g(u_{t+k}, u_{t+k-1}, \cdots)$$

where the prediction of y_{t+k} does not use any information of the past outputs, i.e. there is no correction from the measurement of the output. This predictor is equivalent to

$$\hat{y}_t = g(u_t, u_{t-1}, \cdots)$$

which is exactly a simulator. Infinite step ahead prediction is also known as simulation. Model validation using infinite step ahead prediction is a more rigorous validation of dynamic models if the objective of modeling is toward a true model.

CYTOTOXICITY EXPERIMENTS

Experiment Setup

The RT-CES system (ACEA Biosciences, CA, USA) has been used for this study. The RT-CES system was described previously in (Xing *et al.*, 2005). Briefly, it consists of a 16x microelectronic sensor devices having 16 plastic wells in microtiter plate format, a device station and an electronic sensor analyzer. Cells will be grown onto the surfaces of microelectronic sensors. In operation, the sensor devices with cultured cells will be mounted to a device station placed inside a CO_2 incubator. Electrical cables will connect the device station to the sensor analyzer. Under the control of RT-CES software, the sensor analyzer will automatically select wells to be measured and continuously conduct measurements on wells. The electronic impedance can then be transferred to a computer and recorded.

A parameter termed CI is derived to represent cell status based on the measured electrical impedance. The frequency dependent electrode impedance (resistance) without or with cells present in the wells is represented as $R_b(f)$ and $R_{cell}(f)$, respectively. The CI is calculated by

$$CI = \max_{i=1,\ldots,N}[\frac{R_{cell}(f_i)}{R_b(f_i)} - 1]$$

where N is the number of the frequency points at which the impedance is measured. Several features of the CI can be derived: (i) Under the same physiological conditions, if more cells attach onto the electrodes, the larger impedance value leading to a larger CI value will be detected. If no cells are present on the electrodes or if the cells are not well-attached onto the electrodes, $R_{cell(f)}$ is the same as $R_b(f)$, leading to CI = 0. (ii) A large $R_{cell}(f)$ value leads to a larger CI. Thus, CI is a quantitative measure of the number of cells attached to the sensors. (iii) For the same number of cells attached to the sensors, changes in cell status, such as morphological change, will lead to a change in CI.

Except for cell numbers, the impedance also depends on the extent to which cells attach to the electrodes. For example, if cells spread, there will be a greater cell/electrode contact area, resulting in larger impedance. Thus, the cell biological status including cell viability, cell number, cell morphology, and cell adhesion will all affect the measurement of electrode impedance that is reflected by cell index (CI) on the RT-CES system. Therefore, a dynamic pattern of a given CI curve can indicate sophisticated physiological and pathological responses of the living cells to a given toxic compound (Xing *et al.*, 2005).

Three environmental toxicants, sodium arsenite [As (III)], mercury (II) chlo-

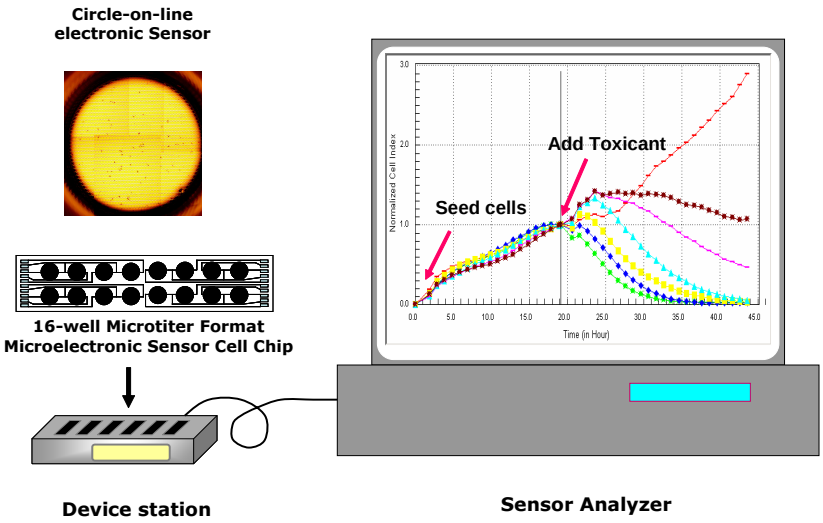

Fig. 1. The RT-CES system and cytotoxicity experiment.

ride, and sodium dichromate [chromium (VI)], were used for cytotoxicity assessment on the 16 sensor device. The cell line NIH 3T3 was tested. The starting cell number was 10000 cells per sensor wells. The cell growth on the sensor device was monitored in real time by the RT-CES system. When the CI values reached a range between 1.0 and 1.2, the cells were then exposed to either As(III), mercury(II) chloride, or chromium(VI) at different concentrations. After compound addition, the cell responses to the compounds were continuously and automatically monitored every hour by the RT-CES system. The schematic diagram of the instrument for cytotoxicity experiments is shown in Fig.1.

Dynamic Growth With Toxicity

In the cytotoxicity experiments the NIH 3T3 cells were treated with As (III), mercury (II) chloride, and chromium (VI), respectively, at different concentrations. After treatment, the CI was recorded in real time every hour for up to 24 h. Notably, the dynamic CI patterns of the NIH 3T3 cells in response to three toxicants are distinct and shown in Fig.2.

The left panel of Fig 2 shows dynamic cytotoxic response to different doses of As (III). The data in the figure indicates that, higher dose toxicant yields, smaller CI at the steady state, as expected. Cells treated with As (III) showed a significant but transient increase in the CI during the first 5 h after the treatment, this phenomenon has been explained as cell fusion (Xing *et al.*, 2005), followed by gradually declining in the CI induced by cell apoptosis. The middle panel shows dynamic cytotoxic response to different doses of chromium (VI). Chromium (VI) triggered cell apoptosis so that the initial cell killing is

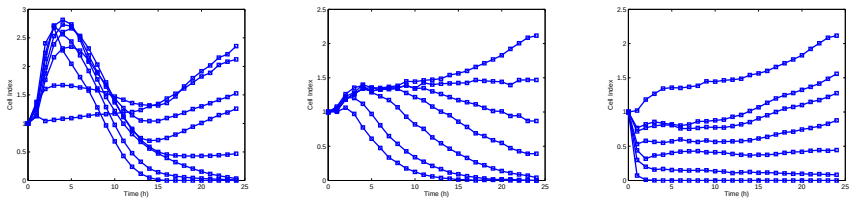

(a) As(III) (b) Chromium (c) Mercury

Fig. 2. *Dynamic responses of cells to As (III), mercury, and chromium(VI). NIH 3T3 cells were seeded into the 16x sensor device, and cell proliferation was then monitored. Once the cells entered the exponential growth phase, cells were treated with As (III), mercury, or chromium(VI) at different doses as indicated. The cytotoxicity was then monitored dynamically. Left panel is the dynamic cytotoxic response to different doses of As (III) in the unit of μM: 0; 1.25; 4.06; 6.21; 9.20; 13.58; 20.01; 29.64. Middle panel is the dynamic cytotoxic response to different doses of chromium(VI): 0; 0.62; 0.91; 1.97; 2.89; 4.25; 5.78. Right panel is the dynamic cytotoxic response to different doses of mercury: 0; 10.43; 15.2; 22.35; 32.8; 48.3; 71.*

relatively slow. Lower doses of chromium (VI) triggered apoptosis slower and the target cells continually grew in early stage inducing a slight initial increase of CI; unlike As (III) however, there is no sharp initial increase of CI. The right panel shows dynamic cytotoxic response to mercury. A quick decrease in the CI with strictly dose-dependence, which occurred at the first hour of the treatment, was induced by mercury that induced cytotoxicity due to quick apoptosis and necrosis mediated by reactive oxygen species with increasing membrane permeability.

The nonlinearity of cytotoxicity is clearly shown by the fact that the responses are bounded (stable) for small doses of the toxicant but unbounded (unstable) for large doses of the toxicant. For example, in left panel of Fig 2, the cytotoxicity response to As(III) is bounded for the doses of 9.20; 13.58; 20.01; 29.64, but unbounded for the rest of the doses. Similar phenomena can be observed for cytotoxicity responses of mercury, or chromium.

NONLINEAR BLACKBOX MODELING

The theory of system identification has been well documented in (Ljung, 1999). The algorithms for nonlinear system identification have also been presented in detail in (Norgaard *et al.*, 2003). In this section, we will focus on the application of nonlinear system identification in cytotoxicity modeling, but not system identification theory and algorithms.

For As (III) experiments, data consist of eight different doses of toxicant in-

cluding one zero dosing, each dose having 25 dynamic data points recorded after the injection of the toxicant with 1hr sampling period. Among the eight experiments corresponding to eight As (III) doses, four of them will be used for nonlinear blackbox modelling (identification data set) and the remaining four for validation (validation data set).

Neural networks with hyperbolic tangent activation functions and NARX model structures are applied to the identification data set, and the dynamic model and parameters are trained through Nonlinear System Identification Toolbox (Norgaard *et al.*, 2003). Through a number of identification trials, the following parameters are found appropriate: 1 hidden layer, 3 nodes, 3rd order lagged input/output (i.e. $y_t, \ldots, y_{t-3}, u_t, \ldots, u_{t-3}$), and zero time delay (owing to large sampling interval). Fig.3 shows comparison of model fit based on one-step ahead prediction, while Fig.4 shows comparison of model fit based on five-step ahead prediction. The left panel is self validation, and right panel is cross validation; the results indicate a good fit of the model if one-step ahead prediction is the criterion for model validation. However, the model performance deteriorates for the five-step prediction, and one can safely expect that prediction performance deteriorates further with increase of prediction horizon. Fig.5 shows comparison of model fit based on simulation (infinite step ahead prediction). One can observe that the estimated model has deteriorated performance no matter in self validation or cross validation, indicating that a good short term prediction does not necessarily mean a good model for long term prediction or for simulation.

Note that in NARX simulation shown in Fig.5, there are no data for the first few points. How many initial data points are missing depends on how many lags of the inputs in the NARX model. As an example, consider a model of the form:

$$\hat{y}_t = a\hat{y}_{t-1} + bu_{t-2}$$

If the available input data are $u_0, u_1, \ldots$, then the first simulated point that can be calculated by the model is $\hat{y}_2$ since

$$\hat{y}_2 = a\hat{y}_1 + bu_0$$

and $\hat{y}_0, \hat{y}_1$ can not be simulated from the model. When calculating $\hat{y}_2$, both $\hat{y}_0$ and $\hat{y}_1$ will be replaced by actual measurements at the first two points. This practice is adopted in this paper.

In terms of k-step ahead prediction, obviously the previous k outputs must be known for the prediction. Therefore, the prediction plots do not have the first k points.

For mercury experiments, data consists of seven different doses of toxicant including one zero dosing, each dose having 25 dynamic data points recorded after the addition of the toxicant with 1hr sampling period. Among the seven

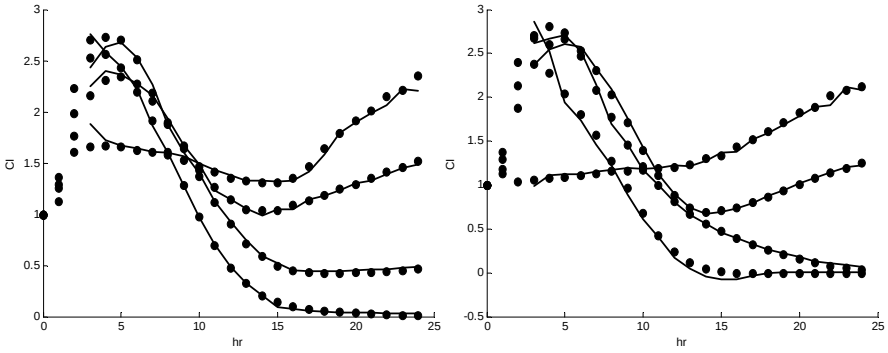

Fig. 3. Model fit based on one-step ahead prediction for As(III) toxicant; solid line is prediction; solid circle is actual measurement of CI; left panel is self validation; right panel is cross validation.

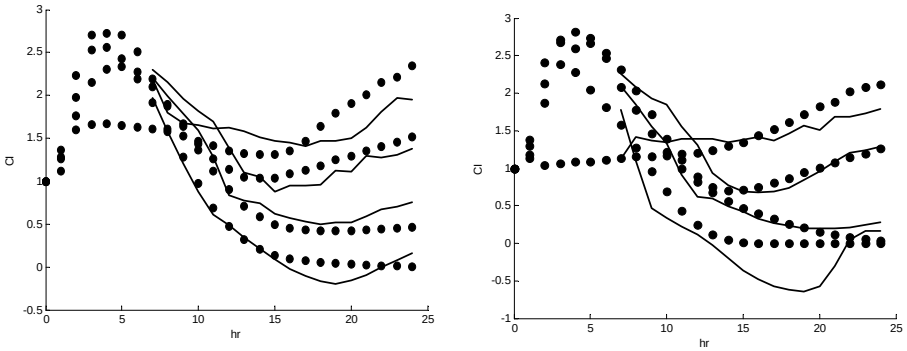

Fig. 4. Model fit based on five-step ahead prediction for As(III) toxicant; left panel is self validation; right panel is cross validation.

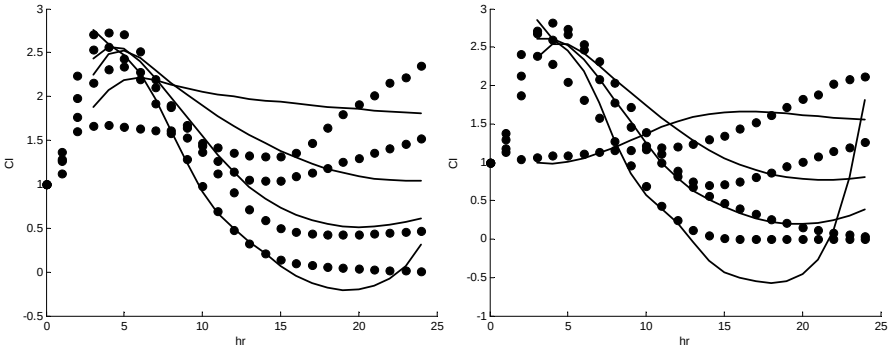

Fig. 5. Model validation based on simulation for As(III) toxicant; left panel is self validation; right panel is cross validation.

experiments corresponding to seven mercury doses, four of them will be used for nonlinear blackbox modeling and the remaining three for validation.

Similar to the As (III) modeling, the NARX model has been applied to the identification data set. Fig.6 shows comparison of model fit based on one-step

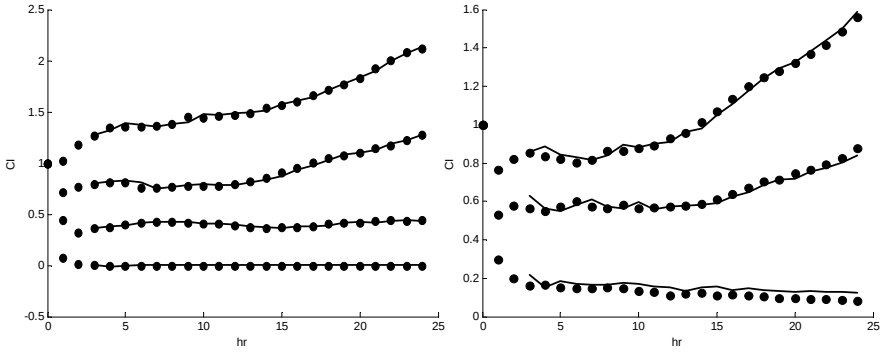

Fig. 6. Model fit based on one-step ahead prediction for mercury toxicant; left panel is self validation; right panel is cross validation.

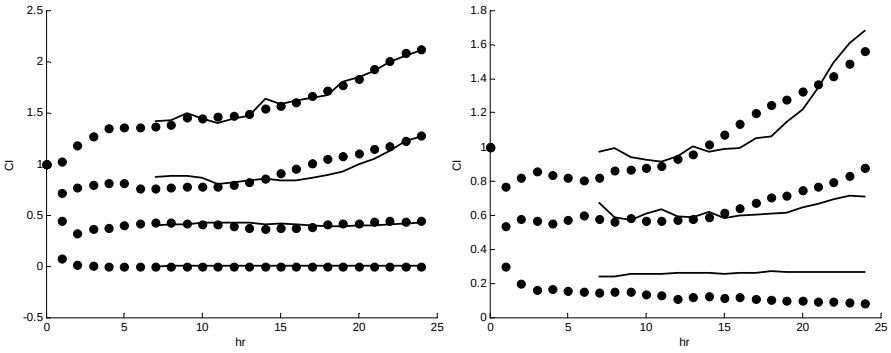

Fig. 7. Model fit based on five-step ahead prediction for mercury toxicant; left panel is self validation; right panel is cross validation.

ahead prediction, while Fig.7 shows comparison of model fit based on five-step ahead prediction. The selection of one and five step predictions here is arbitrary and they are used to indicate the increase of the prediction horizon. As expected, one-step prediction indicates good performance but the five-step prediction does not deteriorate too much in this example. Fig.8 shows comparison of model fit based on simulation. One can observe once again that the estimated model does not have good simulation validation.

For chromium experiments, number of experiments, duration of experiments, and sampling rate are all the same as those of mercury experiments. The NARX model has been applied to the identification data set. Fig.9 and 10 show comparison of model fit based on one-step and five-step ahead predictions, respectively. Fig.11 shows comparison of model fit based on simulation. One can observe that the five-step ahead prediction has similar performance as that of simulation; overall they are reasonable well fitted but some bias is also observed from the simulation plot.

Remark 1 *A number of approaches for improving nonlinear blackbox modeling of cytotoxicity have been tried, including determination of lags in the model*

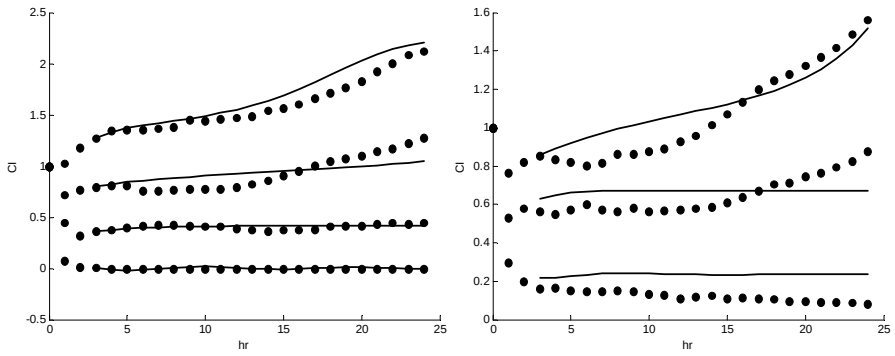

Fig. 8. Model validation based on simulation for mercury toxicant; left panel is self validation; right panel is cross validation.

through a comprehensive search, selection of optimal model structure through regularization, pruning through the optimal brain surgeon algorithm (Norgaard et al.*, 2003). No significant difference in terms of long term prediction or simulation has been observed.*

To summarize, the advantages of blackbox modeling are clearly its simplicity, no priori knowledge of underlying process needed, and good performance in short term prediction. Depending on the dynamics of the process, however, long term prediction can deteriorate quickly. For faster underlying dynamics such as As (III), five-step ahead prediction deteriorates quicker. Both mercury data and chromium data are, however, relatively smooth (slower dynamics), its five-step ahead prediction as well as simulation does not deteriorate as fast as that of As (III). This is expected since all finite step ahead predictions are based on corrections of the available measurements, i.e. there are corrections of future prediction by the current measurements. Smoother the data is, more dependent the future data is on the current data. However, no matter how good fit of the short term prediction, two of the three blackbox models do not seem to have satisfactory simulation tests, indicating that good short term prediction does not mean that the model has captured the true process mechanism. The underling cytotoxicity mechanism is a complex process and appears not to be easily captured by blackbox modeling. To obtain a dynamic cytotoxicity model for long term prediction, the underlying mechanism should be understood, first-principle models should be established, and this is considered in the next section.

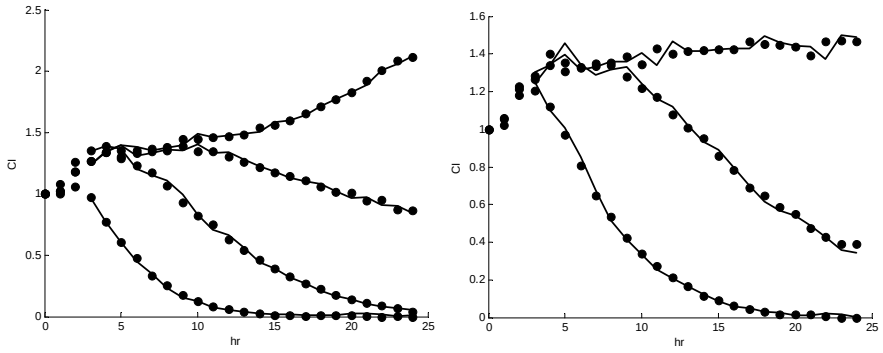

Fig. 9. Model fit based on one-step ahead prediction for chromium toxicant; left panel is self validation; right panel is cross validation.

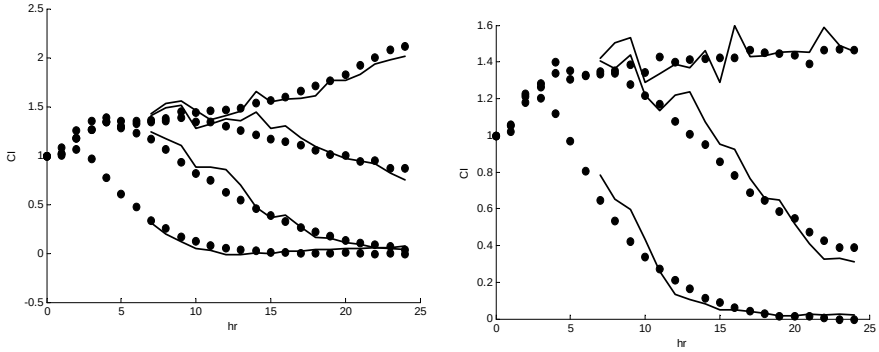

Fig. 10. Model fit based on five-step ahead prediction for chromium toxicant; left panel is self validation; right panel is cross validation.

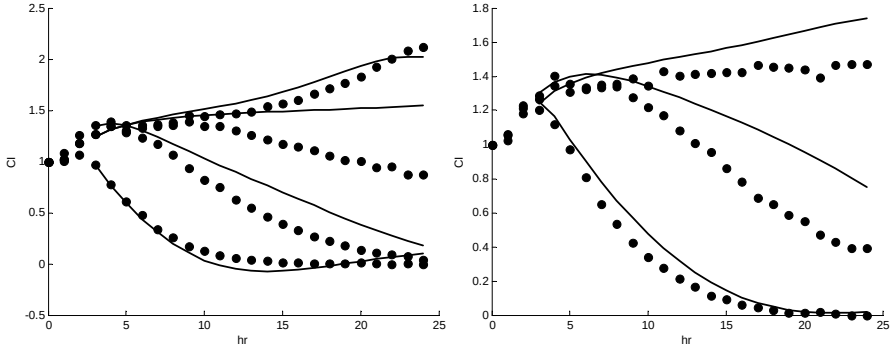

Fig. 11. Model validation based on simulation for chromium toxicant; left panel is self validation; right panel is cross validation.

FIRST-PRINCIPLE MODELING AND PARAMETER ESTIMATIONS

Uptake Mechanism Of Toxicant

Certain assumptions about mechanisms of cytotoxicity in vitro have been considered in literature, which have been discussed in the introduction section.

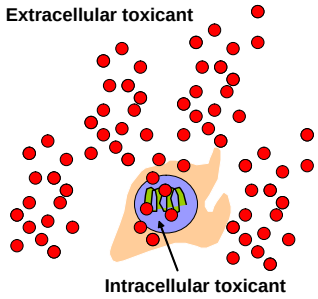

Fig. 12. Transport process of toxicant to cell

They can be summarized as a a two-step process: 1) uptake of toxicant by cells and 2) killing of cells. It has also been pointed out that cells may be killed even before toxicant has entered the cells. In this section, we will investigate two distinct cytotoxicity mechanisms and verify the mechanisms through the cytotoxicity experiments.

The transport process of toxicant into a cell is illustrated in Fig.12. The toxicant uptake dynamics has been discussed in (El-Kareh and Secomby, 2005) where the uptake rate is considered to be a combination of a linear diffusive component and a saturable, carrier-mediated component (Michaelis-Menten like kinetics):

$$\frac{dc_i}{dt} = k_3(k_1 c_e + \frac{k_2 c_e}{K_i + c_e} - c_i) \tag{1}$$

where k_1, k_2, k_3, K_i are constants, and the inclusion of k_1 is for the sake of possible different units between the measurements of intracellular and extracellular concentrations. $k_1 c_e$ reflects the linear diffusive component while $\frac{k_2 c_e}{K_i + c_e}$ is the saturable, carrier-mediated component. This equation is explored further next.

For a given extracellular concentration c_e, integration of eqn.(1) yields

$$c_i = (k_1 c_e + \frac{k_2 c_e}{K_i + c_e})(1 - \exp(-k_3 t)) \tag{2}$$

which has a linear dynamics but is nonlinear in c_e. Note eqn.(2) is valid under the assumption of constant c_e, which is approximately true during the cytotoxicity experiments conducted for this work.

With both intracellular and extracellular toxicant concentrations available, we are ready to develop a dynamic model for cell population dynamics. To this end, we shall understand underlying cytotoxicity mechanism. There are two cell-killing mechanisms by toxicant, namely necrosis and apoptosis, and they are discussed next.

Cytotoxicity Mechanism: Necrosis And Apoptosis

There are two different types of cell death: necrosis and apoptosis. Necrosis is also called "accidental cell death", and can be caused, for example, by a chemical or physical assault to the cell. This event leads to swelling of the cell and disruption of the cell membrane. Organelles, such as the mitochondria or the nucleus, remain intact throughout the process, and all of the cell contents are released into the surrounding tissue. In contrast, apoptosis is a highly regulated process, and is described as programmed cell death. Upon receiving specific signals instructing the cells to undergo apoptosis a number of distinctive biochemical and morphological changes occur in the cell. A family of proteins known as caspases are typically activated in the early stages of apoptosis. These proteins breakdown or cleave key cellular substrates that are required for normal cellular function. The caspases can also activate other degradative enzymes such as DNases, which begin to cleave the DNA in the nucleus. Necrosis causes cell death by direct disrupting cell membrane and cell killing is usually faster than apoptosis. The effects of necrosis mainly depend on the extracellular concentration of the toxicant that affects the cell membrane directly. The effects of apoptosis depend on the intracellular concentration of the toxicant that triggers the signal transduction pathway of apoptosis. The cell killing induced by apoptosis is slower according to activation or synthesis of the proteins in the signal transduction pathway.

In summary, cell killing can go through necrosis, apoptosis, or both. It appears that apoptosis undergoes several more complicated biochemical and morphological processes, and is more challenging in modeling as will be seen shortly.

Cell Population Dynamics

For apoptosis mechanism that mainly depends on intracellular toxicant concentration for cell killing, we consider the rate of cell population given by (Eliaz *et al.*, 2004):

$$\frac{1}{N}\frac{dN}{dt} = (-kc_i + k_s) \tag{3}$$

i.e. the relative cell killing rate in the presence of toxicant is kc_i, and its proliferation rate without the toxicant is k_s.

Substituting eqn.(1) into (3) and then integrating eqn.(1) , we obtain

$$\frac{N(t)}{N_0} = \exp\{[K_4 - (K_1 c_e + \frac{K_2 c_e}{K_5 + c_e})]t\} \exp\{\frac{1}{K_3}(K_1 c_e + \frac{K_2 c_e}{K_5 + c_e})(1 - \exp(-K_3 t))\} \tag{4}$$

where

$$K_1 = kk_1 \; K_2 = kk_2 \; K_3 = k_3 \; K_4 = k_s \; K_5 = K_i$$

Eqn.(4) consists of two exponents. Noting that

$$\lim_{t\to\infty} 1 - \exp(-K_3 t) = 1$$

we see that the second exponent is bounded, i.e.

$$\exp\{\frac{1}{K_3}(K_1 c_e + \frac{K_2 c_e}{K_5 + c_e})(1 - \exp(-K_3 t)\} \leq \exp\{\frac{1}{K_3}(K_1 c_e + \frac{K_2 c_e}{K_5 + c_e})\}$$

The first exponent of eqn.(4) is, however, not necessarily finite. For it to approach zero (i.e. cell to be eventually killed), the following inequality should be satisfied:

$$k_4 - (K_1 c_e + \frac{K_2 c_e}{K_5 + c_e}) < 0 \tag{5}$$

Solving inequality (5) yields the extracellular toxicant concentration needed for the cells to be killed:

$$c_e > \frac{-(K_1 K_5 + K_2 - K_4) + \sqrt{(K_1 K_5 + K_2 - K_4)^2 + 4K_1 K_4 K_5}}{2K_1} \tag{6}$$

This equation shall be useful for the advanced prediction of toxicant killing effect on the cells.

Parameter Estimation And Model Validation For Apoptosis Mechanism

Eqn.(4) contains five unknown parameters and we call it 5-parameter model in the sequel. These parameters can be estimated from experiment data through nonlinear regression.

Chromium(VI) induces apoptosis by p53-dependent or -independent pathways (Bagchi *et al.*, 2001). The chromium-induced gradual cell death has led to the observed CI curves (middle panel of Fig.2) in which the CI values decreased slowly after the toxicant treatment, which were dose-dependent.

The experiment data consists of seven different doses including one zero dosing as discussed previously. Among the seven experiments corresponding to seven chromium doses, four of them will be used for parameter estimation and the remaining three for validation exactly as we did for blackbox modeling.

The estimated parameters for the chromium toxicant are shown in Table 1. The graphic comparisons of model fitting and validation are shown in Fig. 13.

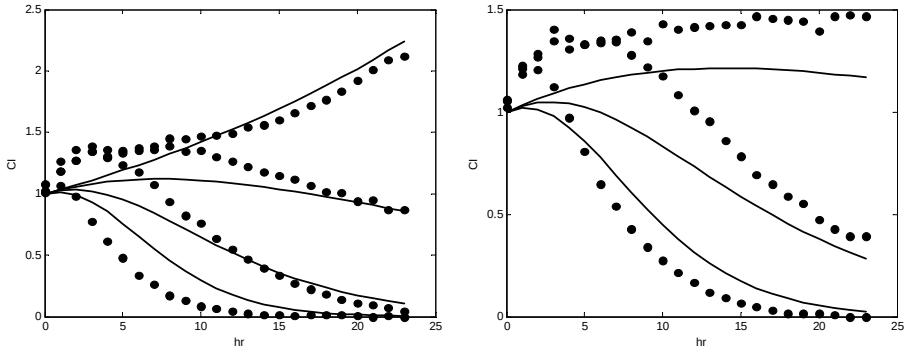

Fig. 13. 5-parameter model validation based on simulation for chromium experiments; left panel is self validation; right panel is cross validation.

Note that the validation shown in Fig. 13 does not use any output measurements to correct the prediction, i.e. it is a validation based on pure simulation. According to 5-parameter model in Table 1, it appears that the Michaelis-Menten uptake is not significant since the estimated K_2 is zero. Thus we may exclude Michaelis-Menten uptake kinetics from the model to yield

$$\frac{N(t)}{N(0)} = \exp\{(K_4 - K_1 c_e)t\} \exp\{\frac{K_1}{K_3} c_e (1 - \exp(-K_3 t))\} \tag{7}$$

We call this model as 3-parameter model. Parameters in eqn.(7) are re-estimated following the same procedure. The three parameters of eqn.(7) are shown in Table 1, where one can see they are very close to their counterparts estimated from the 5-parameter model, indicating no significant Michaelis-Menten uptake in these experiments. Instead, the linear diffusion of toxicant has been the dominant toxicant uptake in these experiments. The comparisons of model fitting and validation are similar to that of 5-parameter model (Fig. 13) and omitted here.

Comparing to blackbox model validation shown in Fig. 11, results in Fig. 13 show a similar performance. The results are overall satisfactory. There is a slight bias in both fits, particularly in the initial response. It has been stated that the initial increase of the cell number is due to the cell fusion process during the initial response of cell to the toxicant, which can occur in apoptosis process (Xing *et al.*, 2005). The lack of fit in the initial phase can certainly propagate into long term fit. Apart from other possible mechanisms in apoptosis that are not known, our model has not considered cell fusion phenomenon as it is not well understood yet, and consequently some mismatch in the model is expected. The difficulty in modeling cell fusion will be elaborated shortly.

Table 1
Parameters estimated

	K_1	K_2	K_3	K_4	K_5
5 parameter model	0.078	0.000	0.093	0.035	4.687
3 parameter model	0.077	N/A	0.094	0.035	N/A

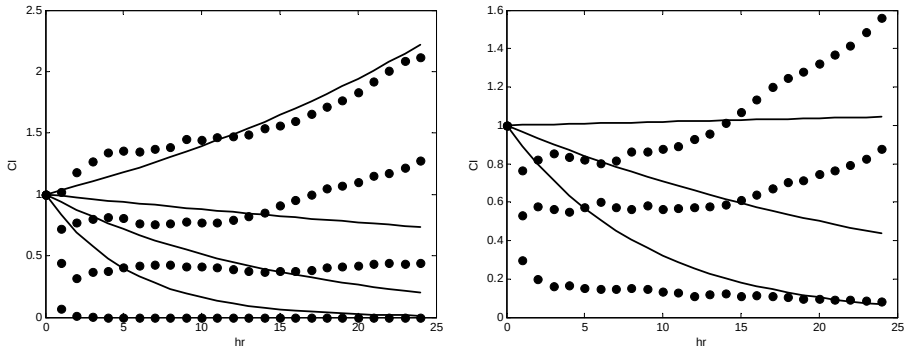

Fig. 14. 5-parameter model validation based on simulation for mercury experiments; left panel is self validation; right panel is cross validation.

For mercury experiments, the right panel of Fig.2 shows that mercury caused a sharp initial decrease in the CI, which occurred at the first hour of the treatment and was strictly dose-dependent. Mercury-induced cytotoxicity is due to apoptosis and necrosis mediated by reactive oxygen species with increasing membrane permeability (Kim and Sharma, 2003; Herr *et al.*, 1981) . The quick drop of the CI values in cultured cells treated with mercury appears to reflect the cell necrosis and quick apoptosis, which is consistent with the previous reports (Kim and Sharma, 2003; Herr *et al.*, 1981).

Thus, the mercury induces mainly the necrosis mechanism but also apoptosis to some extent and the 5-parameter model appears not to be valid. Nevertheless, as a test the 5-parameter model, eqn.(4), has also been applied to the mercury data. The results are shown in Fig.14, where we can see a poor fit of the data, confirming that an incorrect mechanism has been assumed. By visualizing Fig.14, it is clear that the initial killing of cells is quite fast while the 5-parameter model can not achieve this fast dynamics initially since it depends on intracellular toxicant concentration only. The intracellular cellular concentration follows the first order dynamics, eqn.(2), where immediate increase of intracellular concentration is not possible.

As we have already known, with mercury as toxicant, the cell experiences

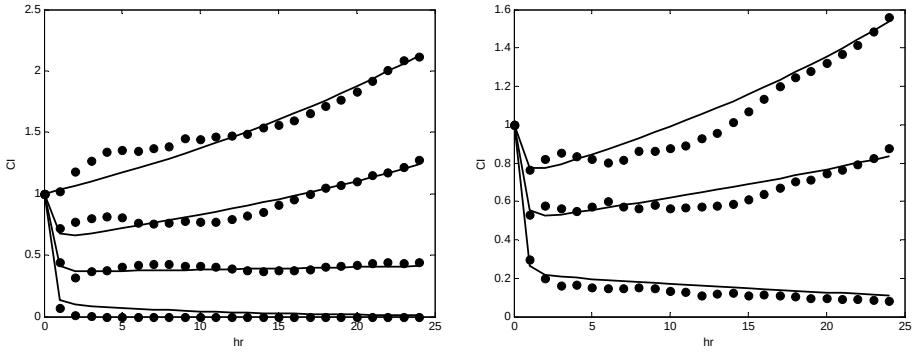

Fig. 15. 6-parameter model validation based on simulation for mercury experiments; left panel is self validation; right panel is cross validation.

Table 2
Parameters estimated

	K_1	K_2	K_3	K_4	K_5	K_6
6 parameter model	0.332	1.897	2.139	0.031	37.07	-0.381

mainly a necrosis process plus a quick apoptosis. Therefore, the cell killing rate depends on both intracellular toxicant and extracellular toxicant. Thus, instead of eqn.(3), consider a cell population dynamics:

$$\frac{dN}{dt} = f(c_i, c_e)N \tag{8}$$

where $f(c_i, c_e)$ is an unknown nonlinear function. As a first order approximation, it is written as

$$\frac{dN}{dt} = (a_0 + a_1 c_i + a_2 c_e)N \tag{9}$$

Now combining (9) with (2), after integration, yields

$$\frac{N(t)}{N(0)} = \exp\{[K_4 + (K_1 + K_6)c_e + \frac{K_2 c_e}{K_5 + c_e})]t\} \exp\{-\frac{1}{K_3}(K_1 c_e + \frac{K_2 c_e}{K_5 + c_e})(1 - \exp(-K_3 t))\} \tag{10}$$

where

$$K_1 = a_1 k_1 \; K_2 = a_1 k_2 \; K_3 = k_3 \; K_4 = a_0 \; K_5 = K_i \; K_6 = a_2$$

This model is called 6-parameter model in the sequel. Now applying the 6-parameter model, eqn.(10), to the mercury data. The results are shown in Fig.15. Comparing to the 5-parameter model shown in Fig.14, a clear improvement of the model has been observed, indicating a more appropriate underlying cytotoxicity mechanism has been found. By comparing with the performance of the blackbox model shown in Fig.8, a dramatic improvement is observed.

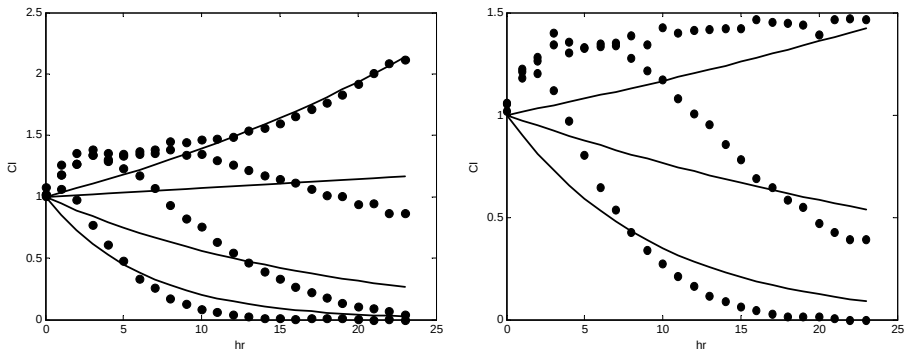

Fig. 16. 6-parameter model validation based on simulation for chromium experiments; left panel is self validation; right panel is cross validation.

A natural question is whether the 6-parameter model can also improve the simulation performance of chromium experiments in which the apoptosis mechanism has played the role. By applying the 6-parameter model to the chromium data, the model validation results are shown in Fig.16. By comparing with the 5-parameter validation shown in Fig.13 one can see that the 6-parameter model does not help, confirming a non-necrosis mechanism of chromium as a toxicant.

Cell Fusion Mechanism

Both 6-parameter model and 5-parameter model are limited to modeling cell killing dynamics. The mechanism of initial cell fusion shown in As (III) experiments (and partially shown in chromium experiments) has not been well understood and thus has not been included in the models.

To show this, applying the 6-parameter model to As (III) data anyway yields results shown in Fig.17. Clearly, the 6-parameter model can not capture the cytotoxicity of As (III), and its performance is worse than that of the blackbox model shown in Fig.5.

The initial cell fusion occurred in apoptosis has not been reported until very recently and its mechanism remains largely unknown (Xing *et al.*, 2005) . In a analysis of As(III) experiments, it was observed through confocal microscope (Xing *et al.*, 2005) that after 3 h of As(III) treatment, individual NIH 3T3 cells fused together forming huge multinuclear cell bodies. The multinuclear cells began to dissociate into smaller multinucleated cells after 8 h of compound addition. These cells appeared to be undergoing nuclear condensation and showed the morphology of the early stage of nuclear fragmentation. After 23 h of As(III) treatment, only a few cells can be detected. The most cells treated with As(III) died most likely through apoptosis. The As(III)-induced

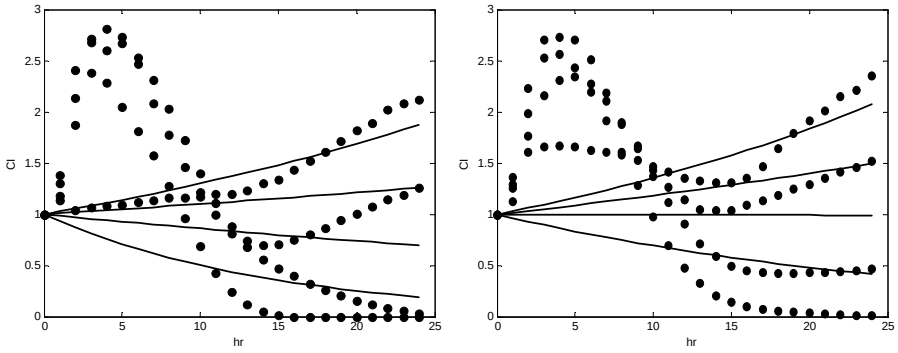

Fig. 17. 6-parameter model validation based on simulation for As (III) experiments; left panel is self validation; right panel is cross validation.

cell fusion increased electrode impedance and resulted in higher CI. Thus, in addition to the need for further confirmation of cell fusion mechanism, any mechanistic modeling of As(III) cell killing needs to consider geometry of cells, nuclear condensation, nuclear fragmenation, and apoptosis simultaneously.

In summary of this section, one can see that the advantage of the first-principle modeling for the cytotoxicity is the significant improvement of the model if the underlying mechanism is truly captured. However, the complexity results if there exist some unknown (or not well known) mechanisms. In contrast, blackbox modeling does not have this limitation. It can fit a model without understanding the underlying mechanism such as the modeling of As (III) experiments, but typically has poor performance in long term prediction and simulation. Therefore, the blackbox modeling and first-principle modeling are not mutually exclusive. Both should be considered in challenging modeling tasks such as the cytotoxicity modeling. Specifically, as far as the underlying cytotoxicity mechanism is known, we have achieved a significantly better model for the necrosis induced cytotoxicity by using first-principle modeling than the blackbox modeling, but the same conclusion does not apply to the apoptosis induced cytotoxicity model. In fact, if there is significant initial cell fusion, then the blackbox approach gives a better model.

CONCLUSION

In this paper, we have considered dynamic modeling of cytotoxicity. The CI data from a real-time cell electronic sensing (RT-CES) system have been used for dynamic modeling. Two types of modeling approaches have been considered, namely blackbox nonlinear dynamic modeling and first-principle modeling plus parameter estimation. The developed models are verified using data that do not participate in the modeling. It has been observed that the balckbox type of nonlinear models can provide a good short term prediction but

may fail long term prediction and simulation; the first-principle model plus parameter estimation does provide a significantly improved dynamic models for long term prediction as well as simulation of cytotoxicity if the underlying mechanism is truly captured in the model structure. The latter models can also provide certain parameters that are useful for prediction such as the necessary doses for cell killing. However, some phenomena observed in cytotoxicity experiments, such as initial cell fusion, have not been well understood and can not be explained from first-principle models. For the modeling discussed in this paper, we find that the necrosis mechanism can be modelled well by the first-principle approach, while the apoptosis mechanism has been modelled better by the blackbox model. Our conclusion is that the blackbox modeling and first-principle modeling are not mutually exclusive. Both should be considered in challenging modeling tasks such as the cytotoxicity problem.

Acknowledgements

This work is supported in part by Natural Sciences and Engineering Research Council of Canada.

References

Bagchi, D., M. Bagchi and S.J. Stohs. Chromium (vi)- induced oxidative stress, apoptotic cell death and modulation of p53 tumor suppressor gene. *Mol. Cell. Biochem.* **222**, 149–158 (2001).

Bar-Joseph, Z. Analyzing time series gene expression data. *Bioinformatics* **20**(16), 2493–2503 (2004).

Doroshow, J.H. Anthracyclines and anthraincendiones.. In: *Cancer Chemotherapy and Biotherapy* (B.A. Chabner and D.L. Longo, Eds.). 2nd ed. pp. 409–434. Lippincott-Raven: Philadelphia, PA. (1996).

El-Kareh, A.W. and T.W. Secomby. Two-mechanism peak concentration model for cellular pharmacodynamics of doxorubicin. *Neoplasia* **77**, 705–713 (2005).

Eliaz, R.E., S. Nir, C. Marty and Jr. F.C. Szoka. Determination and modeling of kinetics of cancer cell killing by doxorubicin and doxorubicin encapsulated in targeted liposomes. *Cancer Research* **64**, 711–718 (2004).

Gewirtz, D.A. A critical evaluation of the mechanisms of action proposed for the antitumor effects of the anthracycline antibiotics, adriamycin and daunorubicin in the tumor cell. *Biochem Pharmacol* **57**, 727–741 (1999).

Herr, H.W., E.L. Kleinert and W.F. Whitmore. Mercury-induced necrosis of murine renal cell carcinoma. *J. Surg. Oncol.* **185**, 95–99 (1981).

Kim, S.H. and R.P. Sharma. Cytotoxicity of inorganic mercury in murine t and b lymphoma cell lines: Involvement of reactive oxygen species, ca(2+) homeostasis, and cytokine gene expression. *Toxicol. in Vitro* **17**, 385–395 (2003).

Lankelma, J., R.F. Luque, H. Dekker and H.M. Pinedo. Simulation model of doxorubicin activity in islets of human breast cancer cells. *Biochimica et Biophysica Acta* **1622**, 169–178 (2003).

Ljung, L. *System Identification*. 2nd ed.. Prentice-Hall, (1999).

Millenbaugh, N.J., M.G. Wientjes and JLS Au. A pharmacodynamic analysis method to determine the relative importance of drug concentration and treatment time on effect. *Cancer Chemother Pharmacol*, **45**, 265–272 (2000).

Norgaard, M., O. Ravn, N.K. Poulsen and L.K. Hansen. *Neural Networks for Modeling and Control of Dynamic Systems*. Springer Verlag. London, (2003).

Ozawa, S., Y. Sugiyama, Y. Mitsuhashi, T. Kobayashi and M. Inaba. Dependence of the cytostatic effect of adriamycin on drug concentration and exposure time in vitro. *British Journal Of Cancer* **41**, 886–891 (1980).

Soderstrom, T. and P. Stoica. *System Identification*. Prentice Hall International. UK, (1989)

Xing, J.Z., L. Zhu, J.A. Jackson, S. Gabos, X.J. Sun, X. Wang and X. Xu. Dynamic monitoring of cytotoxicity on microelectronic sensors. *Chem. Res. Toxicol.* **18**, 154–161 (2005).